Acta Cryst. (1977). B**33**, 2867–2876

Hydrogen Bond Studies. CXXII. A Neutron Diffraction and $X-N$ Deformation-Electron-Density Study of Dimethylammonium Hydrogen Oxalate, $(CH_3)_2NH_2HC_2O_4$, at 298 K

BY JOHN O. THOMAS

Institute of Chemistry, University of Uppsala, Box 531, *S*-751 21 *Uppsala, Sweden*

(*Received* 21 *February* 1977; *accepted* 10 *March* 1977)

The results of a neutron-diffraction study are combined with earlier X-ray data to give $X-N$ deformation-electron-density maps for the simple hydrogen-bonded structure dimethylammonium hydrogen oxalate [Thomas & Pramatus, *Acta Cryst.* (1975), B**31**, 2159–2161]. The contents of the maps are discussed qualitatively in the context of familiar hydrogen-bond concepts. The maps suggest that the shorter the H···O contact, the less well-developed the region of lone-pair electron density associated with the acceptor O atom in the acceptor direction. Differences in (covalent) bonding electron density are also observed and can again be related to hydrogen-bond features in the structure. Confirmation of the credibility and general validity of these observations must await the accumulated evidence of more and better optimized studies of this type.

Introduction

The current state of the art regarding $X-N$ deformation-electron-density work (see, for example, Coppens & Lehmann, 1976) is that, provided the experiment is carried out at the lowest temperatures feasible and that meticulous attention is paid to all aspects of the data collection and processing, results can be obtained which are (apart from in the immediate vicinity of the nuclei) at least as accurate as those attainable from the best current theoretical calculations for systems of comparable complexity.

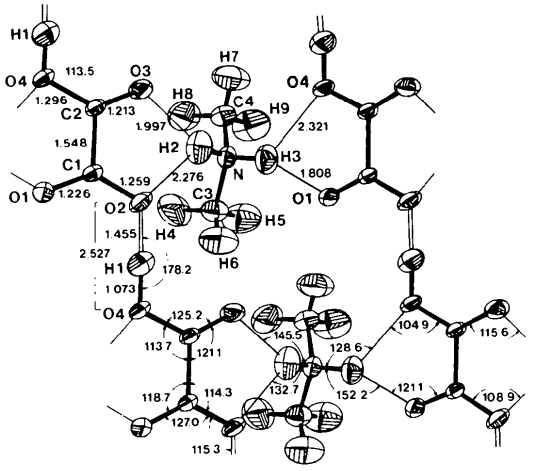

Fig. 1. The detailed geometry as determined by neutron diffraction. Thermal ellipsoids are drawn to include 50% probability. Bond distances and angles have been included where practicable; a more complete list is given in Table 4.

It is valid, nevertheless, to investigate the qualitative credibility of features found in maps obtained from a *less than* optimized experiment, typically one carried out at room-temperature. The question is an important one, since it can often happen that a qualitative picture of the electron distribution is sufficient, provided that we can have faith in its validity. The present study obviously cannot give the complete answer, but it does provide results from a less-than-ideal set of conditions, with which those from a better optimized experiment can later be compared.

The compound studied, dimethylammonium hydrogen oxalate (Fig. 1), is a relatively simple hydrogen-bonded system containing only first and second row elements, and one which an earlier X-ray diffraction study (Thomas & Pramatus, 1975) (hereinafter: TP) suggested could provide useful information relating to the electron density distribution in hydrogen-bonded structures. The major experimental limitation, as indicated above, is that the work has been carried out at ambient temperature (~298 K). It is intended to repeat the experiment at some later date when both low-temperature X-ray and neutron diffraction systems are available. In this way, the effect on the maps of thermal smearing (Ruysink & Vos, 1974) and thermal diffuse scattering (Stevens, 1974) can be minimized.

Crystal data

Dimethylammonium hydrogen oxalate, $(CH_3)_2NH_2HC_2O_4$. Monoclinic, $P2_1/c$, $Z=4$. Cell parameters at 298 K: $a=5{\cdot}630$ (1), $b=9{\cdot}767$ (1), $c=12{\cdot}425$ (1) Å, $\beta=111{\cdot}29$ (1)°, $V=636{\cdot}60$ Å^3, $D_x=1{\cdot}410$ g cm^{-3}, μ_c(Mo $K\alpha$) = 1·36, μ_o(neutron) = 1·48 cm^{-1}.

Experiment and refinement

All essential detail relating to the X-ray part of this investigation has been given in TP. A few points are repeated here, however, which have a particular bearing on the subsequent use of the data to produce $X-N$ deformation-electron-density maps. The data were collected at ~298 K with an automatic four-circle diffractometer ($\omega/2\theta$ scan) and graphite-monochromatized Mo $K\alpha$ radiation ($\lambda = 0{\cdot}71069$ Å) out to sin $\theta/\lambda = 0{\cdot}594$ Å^{-1}, at which point the high-angle data were already becoming rather weak (see *Discussion*). The final data set included 1108 independent reflexions after averaging hkl and $h\bar{k}l$ pairs. Of

Table 1. *Summary of final X-ray and neutron refinements*

Data	$R(F^2)$	$R_w(F^2)$	$R(F)$	Number of reflexions	Number of parameters refined	σ_{X-Y} (Å)	σ_{X-H} (Å)
X	0·049	0·075	0·030	987 ($>2\sigma$)	119	0·002	0·019
N	0·077*	0·089	0·080	1635	169	0·003	0·006
$X-N$	0·115	0·155	0·066	946	1	—	—

* R values excessively high because of the inclusion of all reflexions (see text).

Table 2. *The neutron- and X-ray-diffraction-determined atomic positional parameters* ($\times 10^4$)

The neutron values are given in the upper row. The asphericity shift D is the distance between the neutron- and X-ray-determined-positions; δ is the angular discrepancy between the X-ray- and neutron-determined X–H directions.

	x	y	z	Asphericity shift D (Å)	δ (°)
O(1)	−1642 (4)	1060 (3)	3883 (2)	0·006 (3)	—
	−1645 (2)	1064 (1)	3879 (1)		
O(2)	−1982 (4)	2183 (3)	5377 (2)	0·004 (3)	—
	−1980 (2)	2181 (1)	5379 (1)		
O(3)	3084 (4)	2638 (3)	6183 (2)	0·005 (3)	—
	3083 (2)	2640 (1)	6180 (1)		
O(4)	3329 (4)	1590 (3)	4634 (2)	0·006 (2)	—
	3320 (2)	1590 (1)	4632 (1)		
C(1)	−768 (3)	1707 (2)	4787 (1)	0·002 (2)	—
	−768 (2)	1707 (1)	4785 (1)		
C(2)	2126 (3)	2017 (2)	5283 (2)	0·004 (2)	—
	2120 (2)	2017 (1)	5281 (1)		
N	315 (3)	565 (1)	2175 (1)	0·002 (2)	—
	318 (2)	566 (1)	2174 (1)		
C(3)	−2135 (4)	−51 (2)	1456 (2)	0·004 (3)	—
	−2129 (3)	−49 (2)	1455 (1)		
C(4)	2494 (4)	−375 (2)	2401 (2)	0·006 (3)	—
	2496 (3)	−376 (2)	2397 (1)		
H(1)	5321 (8)	1838 (5)	4965 (4)	0·094 (21)	1·8 (1·2)
	5143 (44)	1847 (18)	4931 (16)		
H(2)	644 (11)	1421 (4)	1769 (4)	0·114 (18)	0·4 (1·0)
	619 (31)	1324 (15)	1817 (12)		
H(3)	157 (9)	846 (5)	2949 (4)	0·134 (12)	1·9 (1·0)
	115 (29)	807 (15)	2841 (14)		
H(4)	−2074 (13)	−313 (8)	631 (5)	0·118 (24)	1·9 (1·3)
	−2013 (35)	−276 (18)	724 (18)		
H(5)	−2451 (12)	−941 (7)	1881 (7)	0·130 (23)	3·5 (1·3)
	−2354 (36)	−876 (20)	1818 (15)		
H(6)	−3617 (11)	689 (7)	1350 (7)	0·092 (22)	1·6 (1·4)
	−3474 (39)	638 (18)	1380 (16)		
H(7)	4222 (10)	149 (7)	2893 (6)	0·136 (24)	5·7 (1·4)
	4103 (43)	109 (19)	2782 (18)		
H(8)	2569 (12)	−693 (8)	1581 (6)	0·113 (24)	1·4 (1·1)
	2596 (34)	−638 (18)	1666 (17)		
H(9)	2204 (13)	−1249 (6)	2854 (7)	0·127 (23)	2·6 (1·4)
	2173 (41)	−1162 (19)	2773 (16)		

these, 121 had intensities less then $2\sigma(I)$. Only an isotropic secondary extinction parameter (g) was refined (Coppens & Hamilton, 1970) to give a final value of 6480 (1010). No attempt was made to correct for TDS or multiple reflexion. Certain details pertaining to the final refinement are summarized in Table 1.

The crystal used in the neutron diffraction study was prepared in the same way as the X-ray crystal. It had a volume of ~27 mm^3.* The data were collected at ~298 K on a PDP-8-controlled Hilger & Watts four-circle diffractometer at the R2 reactor at Studsvik. The double-monochromator-crystal system used to produce the low-background beam of thermal neutrons has been described earlier by Stedman, Almqvist, Raunio & Nilsson (1969). The neutron flux at the crystal was $1{\cdot}26 \times 10^6$ n cm^{-2} s^{-1}, with a mean wavelength of 1·210 Å. The crystal was mounted in a general orientation. All reflexions within a quadrant of reciprocal space were collected out to $\sin\theta/\lambda = 0{\cdot}660$ Å^{-1}; three standard reflexions were monitored at regular intervals as a continuous check on the mechanical stability of the crystal and the electrical stability of the measuring system. After the removal of 'absent' reflexions (collected to confirm the space group), 1679 reflexions remained. Because of the high level of extinction in the data, reflexions of type $0kl$ and $0k\bar{l}$ were not averaged together. Altogether, 162 reflexions had negative intensities and were set equal to $\sigma_{\text{count}}(I)/10$, where $\sigma_{\text{count}}(I)$ is the standard deviation calculated on the basis of Poisson counting statistics. The intensities were corrected for background, Lorentz, absorption and secondary extinction effects (see later). The linear absorption coefficient (μ) was measured experimentally to 1·48 cm^{-1}, corresponding to 25·9 barns for the incoherent scattering cross-section for H. The calculated transmission factors fell in the range 0·62–0·75.

The final positional and thermal parameters from the X-ray study (Table 2 and footnote, this page) were used as starting parameters in the neutron refinement. Isotropic temperature factors were used in the first stages of refinement, going over to anisotropic temperature factors for all atoms as the refinement proceeded. The function minimized in the full-matrix least-squares refinement program *UPALS* was $\Sigma w(|F_o|^2 - |F_c|^2)$, where $w = 1/\sigma^2(F^2)$ and (*a*) $\sigma^2(F^2) = \sigma^2_{\text{count}}(F^2) + (0{\cdot}025F^2)^2$ for $F^2 \geq L$; and (*b*) $\sigma^2(F^2) = \sigma^2_{\text{count}}(F^2) + [0{\cdot}025(2L - F^2)]^2$ for $F^2 < L$, where L is some F^2 value (here 3·0) below which the reflexions can be considered weak. This expression may be seen as a crude means of down-weighting both the strongest and weakest reflexions with respect to reflexions of intermediate intensity. In the final stages of refinement, the suitability of a type 1 or type 2 anisotropic model for extinction (Coppens & Hamilton, 1970) was tested. A type 2 model was ultimately found to provide marginally better agreement factors and standard deviations. The final refined extinction parameters for both type 1 and type 2 models are given in Table 3. In the final refinement the following parameters were varied: 1 scale factor, 54 positional, 108 anisotropic thermal and 6 anisotropic (type 2) secondary extinction parameters. All reflexions (with $F^2 \geq 0$) were included in the refinement, except for 44 strongly extinction-affected reflexions [all 29 reflexions with EXT > 2·60, and those with 1·70 < EXT < 2·60 for which $(F_o^2 - F_c^2) \lesssim -3\sigma(F^2)$, where $\text{EXT} = F_o^2/F_{\text{obs}}^2$].

The final agreement factors are given in Table 1. The corresponding $R(F^2)$, $R_w(F^2)$ and $R(F)$ values for an identical refinement but omitting 605 observations with $F^2 < 3\sigma(F^2)$ were somewhat lower: 0·062, 0·080 and 0·041, respectively; the standard deviations were, on average, 20% higher from the latter refinement, however.

A normal ΔR probability plot (Abrahams & Keve, 1971) after the final refinement had a slope of 1·18 and an intercept at −0·04. The corresponding values for a plot of only reflexions with EXT < 1·17 were 1·02 and 0·08, respectively.

The coherent neutron scattering amplitudes used in the refinements were: $\bar{b}_O = 5{\cdot}80$, $\bar{b}_N = 9{\cdot}40$, $\bar{b}_C = 6{\cdot}65$ and $\bar{b}_H = -3{\cdot}74$ fermi (Bacon, 1972).

The final positional parameters are given in Table 2, along with the corresponding X-ray values.*

All calculations in the present study have been made with the use of a system of programs described by Lundgren (1976).

* See footnote opposite.

* The crystal's dimensions, orientation matrix and the lists of neutron structure factors, X-ray and neutron anisotropic thermal parameters and r.m.s. components of thermal displacement have been deposited with the British Library Lending Division as Supplementary Publication No. SUP 32629 (15 pp.). Copies may be obtained through The Executive Secretary, International Union of Crystallography, 13 White Friars, Chester CH1 1NZ, England.

Table 3. *Refined values of the anisotropic type* 1 (Z'_{ij}) *and type* 2 (W'_{ij}) *secondary extinction parameters as defined by Coppens & Hamilton* (1970)

Z'_{11}	Z'_{22}	Z'_{33}	Z'_{12}	Z'_{13}	Z'_{23}
23 (2)	26 (4)	10 (1)	20 (4)	0 (2)	−1 (3)
W'_{11}	W'_{22}	W'_{33}	W'_{12}	W'_{13}	W'_{23}
0·081 (9)	0·051 (5)	0·040 (4)	0·057 (10)	−0·021 (6)	−0·039 (7)

Calculation of $X-N$ Fourier synthesis

The earlier X-ray data (TP) and the positional and thermal parameters derived from the present neutron study can be combined to produce a Fourier synthesis of $\rho_{X-N}(\mathbf{r})$, the so-called deformation electron density in the structure. This is done with the expression (for a centrosymmetric structure):

$$\rho_{X-N}(\mathbf{r}) = \frac{2}{V} \sum_{\mathbf{H}} [sF_{o,X}(\mathbf{H}) - F_{c,N}(\mathbf{H})] \cos 2\pi(\mathbf{H} \cdot \mathbf{r}),$$

where $F_{o,X}(\mathbf{H})$ is the observed X-ray structure factor corrected for extinction, $F_{c,N}(\mathbf{H})$ is the X-ray structure factor calculated with the neutron-diffraction-determined structure and the spherical neutral-atom form factors described in TP. The value of the scale factor s used in the difference-Fourier summation is calculated.

As in the study of $LiHCOO.H_2O$ (Thomas, Tellgren & Almlöf, 1975), the summation (and calculation of s) was performed after the removal of various sets of X-ray reflexions. This was done to provide further empirical information on the effect of removing certain reflexion types from an $X-N$ synthesis. Four different syntheses were made after the removal of: (*a*) no reflexions, (*b*) 121 reflexions with $F^2 < 2\sigma(F^2)$, (*c*) 34 reflexions with $\mathrm{EXT}(F^2) > 1{\cdot}03$, (*d*) 155 reflexions of type (*b*) or (*c*). The resulting $X-N$ maps in the least-squares plane through the C and O atoms of the HC_2O_4 anion are given in Fig. 2 and are discussed in the following.

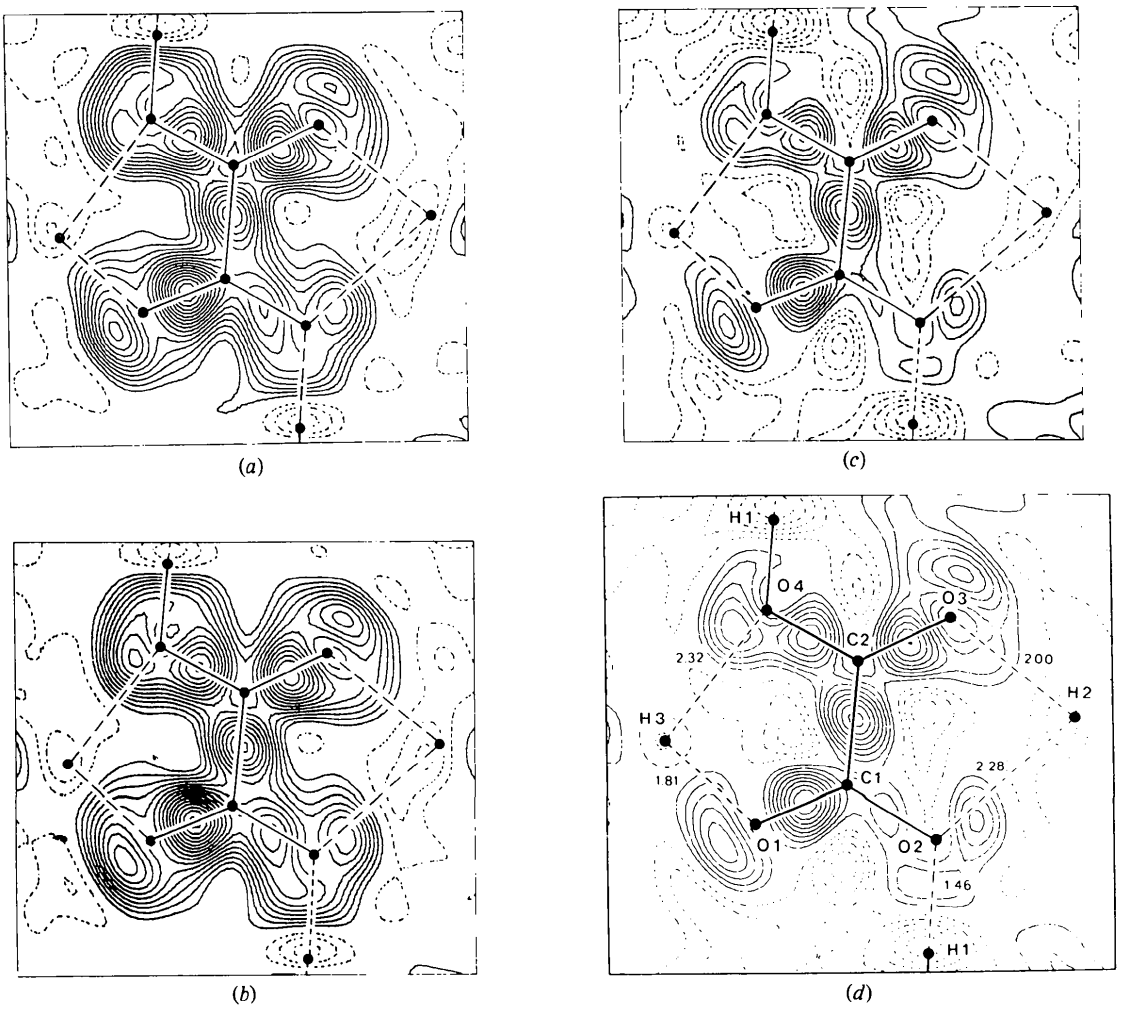

Fig. 2. $X-N$ maps in the least-squares plane through the heavy atoms of the $HC_2O_4^-$ ion calculated with the omission from the X-ray data-set of: (*a*) no reflexions, (*b*) reflexions with $F^2 < 2\sigma(F^2)$, (*c*) reflexions with $\mathrm{EXT}(F^2) > 1{\cdot}03$ and (*d*) reflexions of type (*b*) or (*c*). Here and elsewhere, contour intervals are 0·05 e Å^{-3} and the zero-level contour has been removed. Note also that in (*d*) the difference density at O(3) is zero.

Results and discussion

The general structure

A stereoscopic illustration of the structure as determined by X-ray diffraction appears as Fig. 1 of TP. Distances and angles from the present study are given in Fig. 1, and compared with the X-ray-determined geometry in Table 4. The structure comprises $HC_2O_4^-$ ions linked by the strongest hydrogen bond in the system to form infinite chains running along **a**. These chains are themselves linked transversely by means of N–H···O hydrogen bonds from the cations to produce interlocking puckered layers perpendicular to the *b* axis, the puckering within the layers occurring at the C(3)–N–C(4) angle.

Details of the hydrogen-bond scheme were necessarily somewhat ill-defined from the X-ray study. The present neutron study shows, however, that the two situations suggested earlier as possible bifurcations can, in fact, both justifiably be regarded as such. Each comprises a dominant N–H···O bond [N–H(2)···O(3) and N–H(3)···O(1): H···O distances 1·997(5) and 1·808(5) Å respectively] and a weaker H···O interaction [H(2)···O(2) and H(3)···O(4) distances: 2·276(5) and 2·320(5) Å respectively]. The upper H···O distance limit suggested recently as being commensurate with a genuine hydrogen-bond interaction is 2·4 Å (Olovsson & Jönsson, 1976). Both longer H···O distances thus fall just within this limit.

A further interesting geometrical feature to emerge is that the $(CH_3)_2NH_2^+$ cation has close to *mm* point symmetry; H(6) lies only −0·02 Å and H(7) only +0·05 Å out of the plane defined by C(3)–N–C(4).

Table 4. *Distances and angles in* $(CH_3)_2NH_2HC_2O_4$ *obtained from X-ray and neutron refinements*

The transformations implied by the superscripts are the following:

(i)	$1+x$,	y,	z;	(iv)	$1+x$,	y,	z
(ii)	x,	$\frac{1}{2}-y$,	$-\frac{1}{2}+z$;	(v)	$-x$,	$-y$,	$1-z$
(iii)	$-1+x$,	$\frac{1}{2}-y$,	$-\frac{1}{2}+z$;				

(*a*) $(CH_3)_2NH_2^+$	X-ray	Neutron
N–C(3)	1·471 (2) Å	1·472 (2) Å
N–C(4)	1·476 (2)	1·475 (2)
N–H(2)	0·91 (2)	1·027 (5)
N–H(3)	0·91 (2)	1·035 (4)
C(3)–H(4)	0·96 (2)	1·070 (7)
C(3)–H(5)	0·96 (2)	1·065 (7)
C(3)–H(6)	0·99 (2)	1·075 (7)
C(4)–H(7)	0·98 (2)	1·072 (6)
C(4)–H(8)	0·97 (2)	1·081 (7)
C(4)–H(9)	0·95 (2)	1·067 (7)
C(3)–N–C(4)	113·0 (1)°	113·1 (2)°
H(2)–N–H(3)	110 (1)	109·4 (4)
H(4)–C(3)–H(5)	109 (2)	110·4 (6)
H(4)–C(3)–H(6)	112 (2)	109·7 (6)
H(5)–C(3)–H(6)	113 (2)	110·4 (6)
H(7)–C(4)–H(8)	103 (2)	109·6 (6)
H(7)–C(4)–H(9)	117 (2)	111·3 (6)
H(8)–C(4)–H(9)	110 (2)	109·4 (7)
(*b*) $HC_2O_4^-$		
C(1)–O(1)	1·226 (2) Å	1·226 (3) Å
C(1)–O(2)	1·260 (2)	1·259 (3)
C(1)–C(2)	1·545 (2)	1·548 (2)
C(2)–O(3)	1·214 (2)	1·213 (3)
C(2)–O(4)	1·295 (2)	1·296 (3)
O(4)–H(1)	0·99 (2)	1·073 (4)
O(1)–C(1)–O(2)	127·0 (1)°	127·0 (2)°
O(1)–C(1)–C(2)	118·7 (1)	118·7 (2)
O(2)–C(1)–C(2)	114·2 (1)	114·3 (2)
O(3)–C(2)–O(4)	125·1 (1)	125·2 (2)
O(3)–C(2)–C(1)	121·2 (1)	121·1 (2)
O(4)–C(2)–C(1)	113·6 (1)	113·7 (2)
C(2)–O(4)–H(1)	113 (1)	113·5 (3)

Table 4 (*cont.*)

(*c*) Hydrogen bonds

X–H···*Y*		*X*–H (Å)	H···*Y* (Å)	*X*···*Y* (Å)	∠*X*–H···*Y* (°)
O(4)–H(1)···O(2^{i})	*X*	0·99 (2)	1·54 (2)	2·533 (1)	177 (2)
	N	1·073 (4)	1·455 (5)	2·527 (3)	178·2 (5)
N–H(2)···O(2^{ii})	*X*	0·91 (2)	2·36 (2)	3·065 (1)	134 (1)
	N	1·027 (5)	2·276 (5)	3·066 (3)	132·7 (4)
N–H(2)···O(3^{ii})	*X*	0·91 (2)	2·09 (2)	2·900 (1)	148 (1)
	N	1·027 (5)	1·997 (5)	2·902 (3)	145·5 (4)
N–H(3)···O(1)	*X*	0·91 (2)	1·91 (2)	2·766 (1)	157 (1)
	N	1·035 (4)	1·808 (5)	2·766 (3)	152·2 (4)
N–H(3)···O(4)	*X*	0·91 (2)	2·42 (2)	3·072 (1)	128 (1)
	N	1·035 (4)	2·320 (5)	3·074 (3)	128·6 (4)
C(3)–H(6)···O(3^{iii})	*X*	0·99 (2)	2·51 (2)	3·500 (1)	179 (1)
	N	1·075 (7)	2·426 (7)	3·500 (3)	178·0 (6)
C(4)–H(7)···O(1^{iv})	*X*	0·98 (2)	2·47 (2)	3·441 (1)	173 (2)
	N	1·072 (6)	2·377 (6)	3·441 (3)	171·7 (5)
C(4)–H(9)···O(2^{v})	*X*	0·95 (2)	2·54 (2)	3·377 (1)	147 (1)
	N	1·067 (7)	2·425 (8)	3·376 (4)	147·9 (6)

Comparison of X-ray and neutron-determined parameters

The differences between the positional parameters obtained from the two studies (as illustrated by the asphericity shifts given in Table 2) follow the general pattern of earlier studies of this type, where the only significant discrepancies arise for the H atoms as a result of the severe polarization of their electron-charge distribution. This causes the characteristic 'shortening' of X-ray determined X–H distances with respect to neutron determined values. On the other hand, the corresponding angular discrepancies, δ, between X-ray and neutron-determined directions (Table 2) are small; the only substantial differences occur for C(3)–H(5) and C(4)–H(7) [3·5(1·3) and 5·7(1·4)° respectively].

Systematic differences appear in the heavy-atom temperature factors: neutron-determined values are significantly and systematically lower than X-ray values. Two factors can be responsible for this. (*a*) In the X-ray refinement, anomalously high temperature factors can result from the inadequacy of the spherical scattering model in describing the effective rest-charge distribution for each atom. This effect represents, in this case, no direct threat to the validity of the subsequent $X - N$ maps. (*b*) In the neutron refinement, anomalously low temperature factors can result from an inadequate extinction correction. A normal probability plot (see *Experiment and refinement*) suggested that such an effect can be present here, and thus have a systematic effect on the appearance of the calculated maps.

The deformation-electron-density maps

(*a*) *The* sin θ/λ *cutoff.* As we saw earlier, the data collection was brought to an end at sin $\theta/\lambda = 0{\cdot}594$ Å^{-1}. This must, in general, be regarded as an unduly low cutoff for $X - N$ purposes. It can be noted, however, that the data were already becoming distinctly weaker as sin θ/λ approached 0·59 Å^{-1}. Under these circumstances, a continuation of the data collection to higher angles adds large numbers of very small terms of low statistical significance to the $X - N$ Fourier summation, thus increasing the noise in the maps (see also Thomas, Tellgren & Almlöf, 1975). The recent careful work of Coppens & Lehmann (1976) on *p*-nitropyridine *N*-oxide at 30 K illustrates this point further: X-ray data, although collected out to sin $\theta/\lambda = 1{\cdot}0$ Å^{-1}, were only used out to 0·75 Å^{-1} in the published $X - N$ maps. Furthermore, an increase in noise was clearly evident in going from a 0·65 to a 0·75 Å^{-1} cutoff. Their work also suggests that relative internal features observed in comparable regions of the structure (lone-pair or covalent bond regions) for a lower cutoff are reliably preserved at a higher cutoff [see their Fig. 2(*b*) and (*c*)]. The implication, and one which is assumed in the present discussion, is that relative qualitative features emerging from the present work are largely insensitive to an extension of the cutoff, and are consequently unlikely to contain artifact effects of using a low cutoff.

(*b*) *The effect of omissions on the* $X - N$ *maps.* As described earlier, the effect of omitting two different reflexion types from the $X - N$ Fourier summation has been investigated (Fig. 2*a–d*). The dominant feature of Fig.2 (*a*) and (*b*) is the high degree of spherical symmetry in the vicinity of the atoms. This effect is not seen in Fig. 2 (*c*) and (*d*), which suggests that the presence of more strongly extinction-affected reflexions results in an incorrect calculation of scale factor. Fig. 2 (*c*) and (*d*) are virtually identical; there is a slight suggestion, however, that the inclusion of weak reflexions increases the noise in the maps. On the basis of this and similar evidence from other sections, reflexions with $F^2 < 2\sigma(F^2)$ and reflexions with EXT-$(F^2) > 1{\cdot}03$ were omitted from the calculation of all further maps shown in this paper. Although such omissions seriously prejudice the quantitative credibility of the maps, it is felt that, in practice, the procedure justifies itself by promoting greater confidence in the relative qualitative features which remain. Only such features will be cited in the discussion.

(*c*) *Accuracy of the maps.* Although a detailed analysis can be made of errors in difference maps

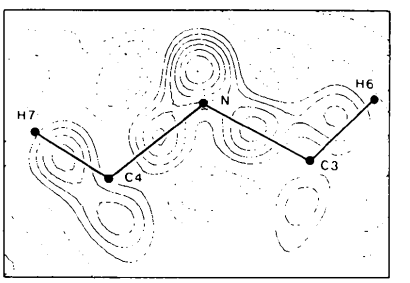

(*a*)

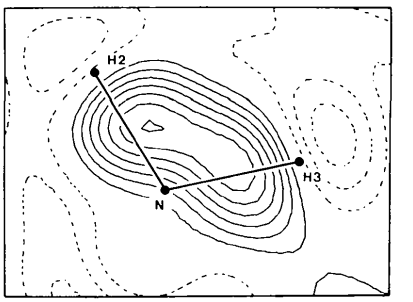

(*b*)

Fig. 3. $X - N$ maps in (*a*) the C(3)–N–C(4) plane and (*b*) the H(2)–N–H(3) plane of the $(CH_3)_2NH_2$ cation. Maps calculated as for Fig. 2(*d*).

(Rees, 1976), such a treatment is not considered meaningful in the present case [see points (*a*) and (*b*) above]. It is convenient, therefore, to have recourse to some feature in the structure where chemical (but *not* crystallographic) considerations require a degree of internal symmetry in the electronic deformation. (Rees has shown, in fact, that the theoretical error function varies dramatically within the maps, having maxima at the atom sites and minima in regions well away from atom centres where, typically, bonding and lone-pair electron density features are to be found.) A chemical symmetry requirement of this type applies in the map given in Fig. 3(*a*): the deformation density associated with the bonds N—C(3) and N—C(4) in the cation should reasonably exhibit a close approximation to mirror symmetry. So is, in fact, the case to a tolerance of less than one contour. An estimate of 0·05 e Å^{-3} for the relative error in the maps at regions away from atom centres would therefore not seem unreasonable. Only features appearing in such regions will be considered hereinafter.

Table 5. *Perpendicular distances, d, from the (least-squares) planes through the non-hydrogen atoms of the cation and anion*

Neutron-determined positional coordinates were used in the calculation

$(CH_3)_2NH_2^+$		$HC_2O_4^-$	
	d (Å)		*d* (Å)
H(2)	0·832 (5)	O(1)	−0·020 (3)
H(3)	−0·850 (5)	O(2)	0·028 (3)
H(4)	0·890 (6)	O(3)	−0·018 (3)
H(5)	−0·862 (8)	O(4)	0·029 (3)
H(6)	−0·023 (8)	C(1)	−0·008 (2)
H(7)	0·047 (7)	C(2)	−0·012 (2)
H(8)	0·870 (7)	H(1)	0·060 (5)
H(9)	−0·882 (8)	H(2)	0·398 (4)
		H(3)	0·377 (5)

Some electron-density aspects of hydrogen bonding

From the wealth of geometrical information available relating to hydrogen-bonded systems, a number of ideas and concepts have evolved which have proved empirically useful in discussing such systems. It is therefore of interest to re-examine some of these concepts as they arise for dimethylammonium hydrogen oxalate in the light of information contained in a set of deformation electron density maps.

(*a*) *Lone-pair directionality.* The implication here is that, on hydrogen-bond formation in a crystal, an energetic compromise is reached in which the lone-pair electrons endeavour to direct themselves toward the active H atoms in the system (or *vice versa*). The directions of the lone-pair lobes are thus seen as playing a decisive role in determining the ultimate structure. A survey made by Jönsson (1973) on the basis of neutron-diffraction-determined geometries reinforces this idea, although molecular-packing considerations clearly become increasingly significant for larger molecules. In this connexion, the deformation electron density associated with the general hydrogen-bond scheme is given in Figs. 2(*d*) and 3. The section taken in Fig. 2(*d*) is the least-squares plane through the 'heavy' atoms of the $HC_2O_4^-$ anion; the distances of the various atoms from this plane are given in Table 5. Sections 0·18 and 0·36 Å above and below this section were also calculated: no peak was substantially reinforced with respect to its magnitude in the least-squares section. General discussions of the present type can thus be concentrated on features observed in the $HC_2O_4^-$ plane.

The lone-pair peaks at the O atoms (Fig. 2*d*) are, with one exception, observed to fall roughly in the 120° position with respect to the C—O bond axis. A similar configuration has been found, for example, in α-glycine (Almlöf, Kvick & Thomas, 1973) and α-glycylglycine (Griffin & Coppens, 1975); all tend to support the general idea of lone-pair directionality. The exceptional case arises for O(1), with a peak near the 180° position. Although such a location has previously been found for the carbonyl O atoms of both benzene chromium tricarbonyl (Rees & Coppens, 1973) and chromium hexacarbonyl (Rees, 1976), no straightforward explanation suggests itself here. That the strong hydrogen bond O(4)—H(1)···O(2) can bring about such a perturbation would seem unlikely, but this cannot be ruled out entirely in view of the much higher peak density found in C(1)—O(1) compared with C(1)—O(2) (0·44 and 0·14 Å^{-3}, respectively). The atom O(1) is also the acceptor of the strongest N—H···O bond from the cation (see below).

The concept of lone-pair directionality becomes more obscure, however, if we consider the relative heights of the lone-pair peaks. Indeed, a distinct correlation would appear to exist between H···O distance and lone-pair electron density in the direction of hydrogen-bond acceptance. Regions of lone-pair difference density in the general direction of strong and intermediate strength hydrogen-bond acceptance appear consistently *weaker* than regions in directions of non-bonding or of weak hydrogen-bond acceptance (Table 6). No integration of the deformation density [of the type made by Staudenmann, Coppens & Muller (1976) for V_3Si] has been attempted; the present aim is merely to draw attention to evidence of a general trend. Indeed, similar evidence was obtained for α-glycine (Almlöf, Kvick & Thomas, 1973), where differences were also observed in the strengths of lone-pair orbital peaks for the terminal oxygen O(1) (Fig. 4). The weaker lobe in the direction of acceptance of the strongest N—H···O bond in the structure (H···O 1·728 Å) reaches only ~0·28 e Å^{-3}; the other lobe in the general direction of

Table 6. *Peak lone-pair difference density in the $HC_2O_4^-$ anion plane in the directions of hydrogen-bond acceptance*

Hydrogen	Acceptor oxygen	H···O (Å)	Peak $\rho_{X-N}(\mathbf{r})$ (e Å^{-3})
H(1)	O(2)	1·46	0·14
H(3)	O(1)	1·81	0·10
H(2)	O(3)	2·00	0·13
H(2)	O(2)	2·28	0·22
H(3)	O(4)	2·32	0·30
[—	O(1)	—	0·29]*
[—	O(3)	—	0·32]*

* Non-acceptance site.

acceptance of a weaker N–H···O bond (H···O 2·365 Å) reaches ~0·42 e Å^{-3}. The H atoms concerned lie 0·28 and 0·76 Å, respectively, out of the carboxylate plane.

A warning, however: the theoretical work of Kollman & Allen (1970) led them to make the observation that 'there is no *one* density redistribution characteristic of a hydrogen bond'. Comparisons between different hydrogen-bond systems can thus be misleading.

(*b*) *Bifurcation.* The geometrical concept of bifurcation has been invoked earlier in the discussion. Fig. 2(*d*) provides a suggestive picture of two bifurcated situations in terms of electron density: the demands of lone-pair directionality as discussed above are met such that lone-pair lobes (one *cis* and one *trans*) from two different O acceptors tend to direct themselves towards the active H atoms, H(2) and H(3).

(*c*) *Criteria for hydrogen bonding.* An extrapolation of the above remarks provokes the idea that the limit of bifurcation (when one of the two H···O contacts is no longer adjudged a hydrogen bond) is reached when the lone-pair lobe in question ceases to be perturbed by the proximity of the H atom. In this latter connexion, the difference electron-density maps for the C(3) methyl group also reveal an interesting situation: the H(6)···O(3) contact distance of 2·426(7) Å lies just beyond the geometrical limit (2·4 Å) quoted earlier for hydrogen bonding. Nevertheless, the deformation electron density associated with H(6) (Fig. 5*b*) is clearly lower than that associated with H(4) and H(5) (Fig. 5*a*); the latter are both H atoms which, on geometrical grounds, cannot be involved in hydrogen bonding. The bonding situation for the C(4) methyl group is less clear (Fig. 5*c*, *d*), but even here the difference density associated with H(8), which cannot participate in hydrogen bonding, is again clearly higher than that for H(7) and H(9).

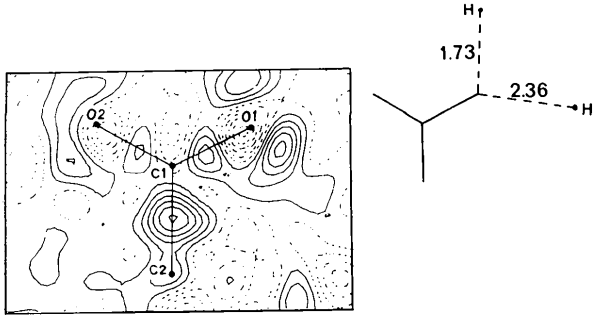

Fig. 4. *X* − *N* map in the plane of the carboxylate group in α-glycine (reproduced from Almlöf, Kvick & Thomas, 1973). Note that here the contour interval is 0·08 e Å^{-3} and the zero-level (first dashed) contour has not been omitted.

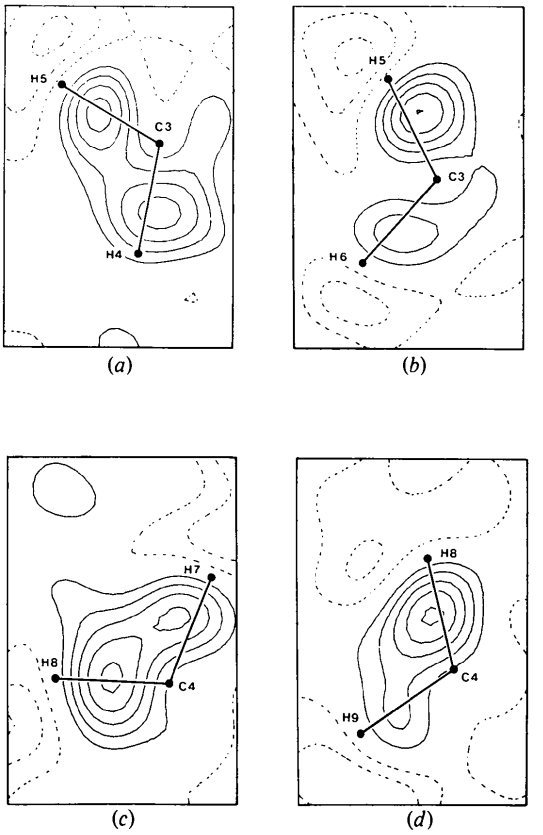

Fig. 5. *X* − *N* maps through various H–C–H planes of the methyl groups: (*a*) H(4)–C(3)–H(5); (*b*) H(5)–C(3)–H(6); (*c*) H(7)–C(4)–H(8); (*d*) H(8)–C(4)–H(9). Maps calculated as for Fig. 2(*d*).

(*d*) *Hydrogen bonding and covalency.* That a hydrogen bond between two molecules can bring about changes in the internal geometries of these molecules is well-known. As an example of this, the effect of hydrogen bonding on C–O lengths in the accepting carboxylate groups of a number of $HC_2O_4^-$ ion chains is

shown in Table 7. The general tendency is towards a greater inequality in C–O bond length the stronger (shorter) the O–H···O bond. In terms of deformation electron density, this is seen for $(CH_3)_2NH_2HC_2O_4$ (Fig. 2*d*) as a significantly lower density in the 'accepting' bond C(1)–O(2) (0·14 e Å^{-3}) than in C(1)–O(1) (0·44 e Å^{-3}). This would suggest that the apparent charge migration away from the O(2)···H(1) lone-pair acceptor site also occurs for the covalent bond C(1)–O(2). That this should qualitatively be so is not unexpected; but it is indeed surprising that the difference between C(1)–O(1) and C(1)–O(2) should be so much greater than that between C(2)–O(3) (0·40 e Å^{-3}) and C(2)–O(4) (0·35 e Å^{-3}), when it is considered that C(2)–O(3) and C(2)–O(4) are expected to exhibit approximately double- and single-bond character respectively. It will be noted that the influence of the weaker N–H···O bonds has been neglected in this particular aspect of the discussion.

Table 7. *The effect of strong hydrogen-bond acceptance on* C–O *bond-lengths in structurally similar carboxylate groups*

The situation in α-glycine is also included for comparison, where only weaker N–H···O bonds are accepted.

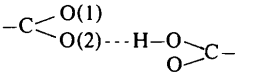

Compound	C–O(1) (Å)	C–O(2) (Å)	O(2)···O (Å)
$(CH_3)_3NHHC_2O_4$	1·218 (3)	1·251 (3)	2·489 (2)
$LiHC_2O_4.H_2O$	1·240 (1)	1·259 (1)	2·490 (1)
$(CH_3)NH_3HC_2O_4$	1·225 (2)	1·252 (2)	2·515 (2)
$(CH_3)_2NH_2HC_2O_4$	1·226 (2)	1·260 (2)	2·533 (1)
$NH_4HC_2O_4.\frac{1}{2}H_2O$*	1·236 (2)	1·257 (2)	2·561 (2)
$NaHC_2O_4.H_2O$	1·242 (2)	1·251 (2)	2·571 (2)
α-Glycine	1·250 (1)	1·251 (1)	—

* Küppers (1973); for other references see Thomas & Renne (1975).

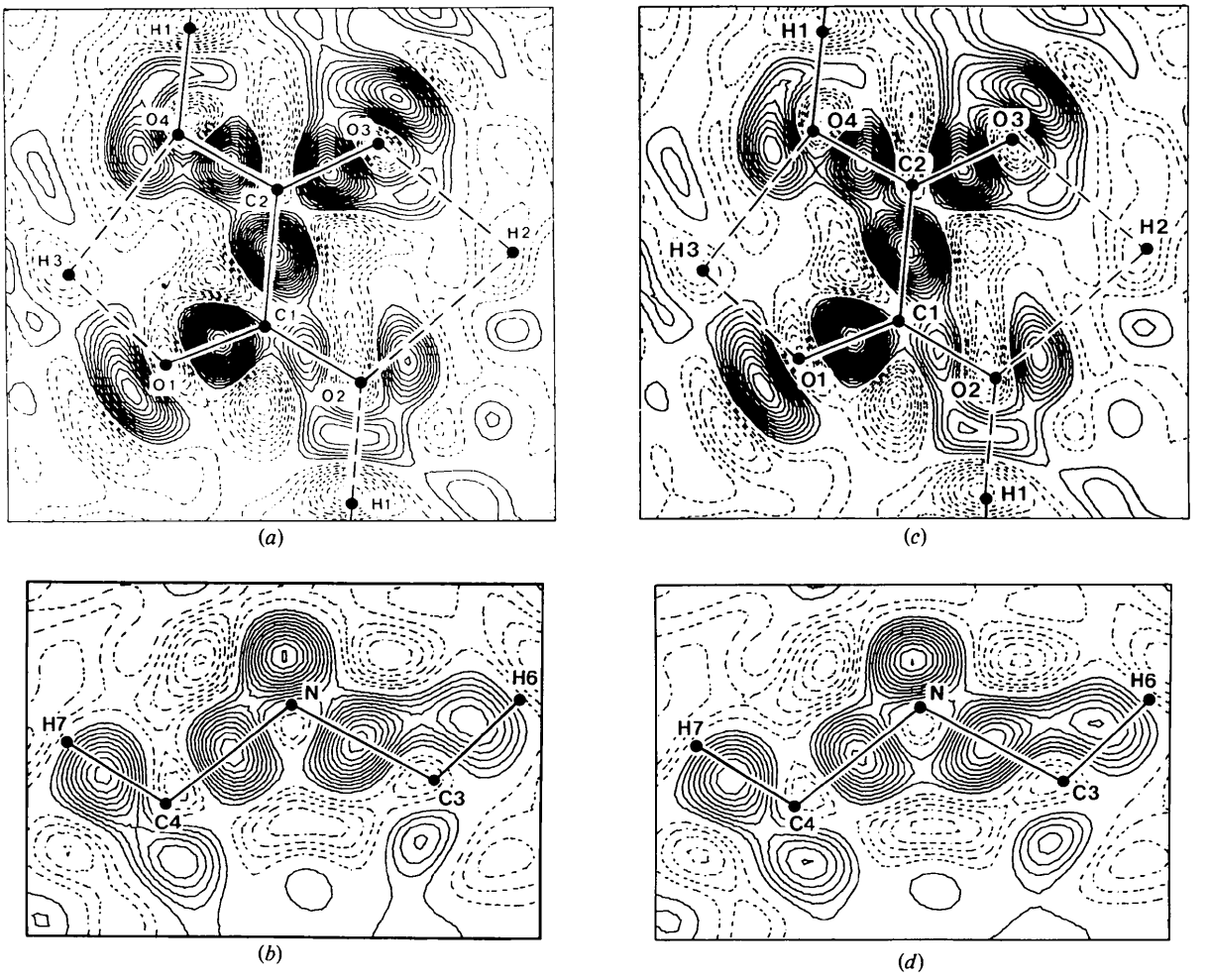

Fig. 6. *X* – *N* maps corrected for thermal smearing: (*a*) and (*b*) are isotropic and (*c*) and (*d*) anisotropic corrections of Figs. 2(*d*) and 3(*a*) (see text). Contour intervals 0·05 e Å^{-3}.

A similar tendency in the C–O bonding electron density has also been found in a recent room-temperature $X-N$ study of $NaHC_2O_4.H_2O$ (Tellgren, Thomas & Olovsson, 1977).

Thermal smearing

The advantage of performing $X-N$ studies at reduced temperatures has been discussed earlier. A crude estimate is made here of the effect of thermal smearing on the present maps. With the neutron-diffraction-determined positional parameters and with the spherical neutral-atom form factors used in the preparation of the maps, a scale factor and overall isotropic ($\bar{B}$) or anisotropic ($\bar{\beta}_{ij}$) temperature factors are refined from the X-ray data. The resulting B value [3·52(8) Å^2] or $\bar{\beta}$ values [$\bar{\beta}_{11}$ = 0·0212 (1), $\bar{\beta}_{22}$ = 0·0116 (3), $\bar{\beta}_{33}$ = 0·0062 (2), $\bar{\beta}_{13}$ = 0·0052 (3)] are then used to apply a thermal sharpening of the coefficients $\Delta F^T(\mathbf{H})$ in the $X-N$ difference Fourier summation such that:

$$\Delta F^\circ(\mathbf{H}) = \Delta F^T(\mathbf{H}) \exp(\bar{B} \sin^2\theta/\lambda^2)$$

or

$$\Delta F^\circ(\mathbf{H}) = \Delta F^T(\mathbf{H}) \exp[\bar{\beta}_{11}h^2 + \bar{\beta}_{22}k^2 + \bar{\beta}_{33}l^2 + 2\bar{\beta}_{13}hl].$$

The effect of these modifications on Figs. 2(*d*) and 3(*a*) is shown in Fig. 6.

The relative qualitative features are reproduced in all four plots with respect to the unmodified room-temperature maps, although the peak heights increase on average (taken over $\bar{B}$ and $\bar{\beta}$ cases) by 102% for $HC_2O_4^-$ and by 94% for $(CH_3)_2NH_2^+$. The anistropic modification reduces the average peak height by 7% with respect to the isotropic case for $HC_2O_4^-$. No net change is found for $(CH_3)_2NH_2^+$.

Temperature-modified $X-N$ maps of this type can usefully be compared with $X-N$ maps measured at low temperatures, or better, with plots of the deformation models refined in a Hirshfeld-type treatment (Hirshfeld, 1971). It must be noted, however, that this type of overall sharpening will not reveal details in the maps which were not already observed at room temperature.

I would like to thank Professor Ivar Olovsson for his unwavering support and encouragement throughout this work. The invaluable help from other members of this Institute is also greatly appreciated. This work is financed by grants from the Swedish Natural Science Research Council; their support is hereby gratefully acknowledged.

References

ABRAHAMS, S. C. & KEVE, E. T. (1971). *Acta Cryst.* A**27**, 157–165.
ALMLÖF, J., KVICK, Å. & THOMAS, J. O. (1973). *J. Chem. Phys.* **59**, 3901–3906.
BACON, G. E. (1972). *Acta Cryst.* A**28**, 357–358.
COPPENS, P. & HAMILTON, W. C. (1970). *Acta Cryst.* A**26**, 71–83.
COPPENS, P. & LEHMANN, M. S. (1976). *Acta Cryst.* B**32**, 1777–1784.
GRIFFIN, J. F. & COPPENS, P. (1975). *J. Amer. Chem. Soc.* **97**, 3496–3505.
HIRSHFELD, F. L. (1971). *Acta Cryst.* B**27**, 769–781.
JÖNSSON, P.-G. (1973). *Acta Univ. Ups.* No. 253.
KOLLMAN, P. A. & ALLEN, L. C. (1970). *J. Chem. Phys.* **52**, 5085–5094.
KÜPPERS, H. (1973). *Acta Cryst.* B**29**, 318–327.
LUNDGREN, J.-O. (1976). *Crystallographic Computer Programs.* UUIC-B13-4-03. Institute of Chemistry, Univ. of Uppsala, Sweden.
OLOVSSON, I. & JÖNSSON, P.-G. (1976). In *The Hydrogen Bond. Recent Developments in Theory and Experiment*, Vol. 2. Edited by P. SCHUSTER, G. ZUNDEL & C. SANDORFY. Amsterdam: North-Holland.
REES, B. (1976). *Acta Cryst.* A**32**, 483–488.
REES, B. & COPPENS, P. (1973). *Acta Cryst.* B**29**, 2515–2524.
RUYSINK, A. F. J. & VOS, A. (1974). *Acta Cryst.* A**30**, 503–506.
STAUDENMANN, J.-L., COPPENS, P. & MULLER, J. (1976). *Solid State Commun.* **19**, 29–33.
STEDMAN, R., ALMQVIST, L., RAUNIO, G. & NILSSON, G. (1969). *Rev. Sci. Instrum.* **40**, 249–255.
STEVENS, E. D. (1974). *Acta Cryst.* A**30**, 184–189.
TELLGREN, R., THOMAS, J. O. & OLOVSSON, I. (1977). *Acta Cryst.* B**33**. In the press.
THOMAS, J. O. & PRAMATUS, S. (1975). *Acta Cryst.* B**31**, 2159–2161.
THOMAS, J. O. & RENNE, N. (1975). *Acta Cryst.* B**31**, 2161–2163.
THOMAS, J. O., TELLGREN, R. & ALMLÖF, J. (1975). *Acta Cryst.* B**31**, 1946–1955.